# 10 Gb/s Multiple Wavelength, Coherent Short Pulse Source Based on Spectral Carving of Supercontinuum Generated in Fibers

Ö. Boyraz, J. Kim, M. N. Islam, *Fellow, OSA*, F. Coppinger, and B. Jalali, *Senior Member, IEEE, Member, OSA*

***Abstract*—We demonstrate a high-power, multi-wavelength, short pulse source at 10 Gb/s based on spectral slicing of supercontinuum (SC) generated in short fibers. We show that short fiber SC can be used for dense wavelength division multiplexing applications because of its >7.9 dBm/nm power spectral density, 140 nm spectral bandwidth, and ±0.5 dB spectral uniformity over 40 nm. Pulse carving up to 60 nm away from the pump wavelength and CW generation by longitudinal mode carving indicates that the coherence of the SC is maintained. By using high nonlinearity fibers, the spectral bandwidth is increased to 250 nm, which can accommodate >600 wavelength channels with 50 GHz channel spacing and >6 Tb/s aggregate data rate. We also calculate the coherence degradation due to amplification of incoherent energy during the SC generation. Theoretical results show that the SC generation in short fibers has 13 dB higher signal-to-noise ratio (SNR) compared to the SC generated in long fiber.**

***Index Terms*—Nonlinear optics, optical fiber communication, optical fiber devices, optical noise, supercontinuum, wavelength division multiplexing (WDM).**

## I. Introduction

DUE TO fast growth in Internet technology, demand for bandwidth is estimated to exceed 1 Tb/s by year 2002 with a further doubling every two years. Utilizing the entire 40 THz low loss transmission window of the silica fibers is one of the ways to answer this growth other than using multiple fiber links. The preferred approach to utilize the low loss transmission window of silica fibers with the current technology is to use the combined techniques of optical time division multiplexing (OTDM) and wavelength division multiplexing (WDM). For a high spectral efficiency, large channel count system, a key enabling technology is a multiple wavelength high repetition rate source with large and uniform bandwidth, accurate wavelength spacing, high coherence, and high-power spectral density.

Dense wavelength division multiplexing (DWDM) sources based on temporal modulation of chirped short pulse lasers have been demonstrated [1], [2]. In this scheme, Knox *et al.* encode the data on different wavelengths by modulating a highly chirped laser spectrum that is temporally distributed. Based on the same scheme, in a recent experiment, Boivin *et al.*have demonstrated 110 channels at 2.35 Gb/s data transmission by utilizing pulse interleaving technique to multiply the repetition rate 64 times [3]. However, the spectral width of the seed pulse and the modulator speed (∼12 GHz) limit the channel count and the pulse width of each channel in this scheme. Moreover, due to the requirement of high chirp rate, it can only operate at higher speeds at the expense of the channel count. Since the power spectral density is not uniform across the spectrum, a special equalization technique is required to obtain uniform wavelength channels. In an alternative scheme, Mikulla *et al.*have demonstrated pulse carving from a laser spectrum broadened in normal dispersion fiber [4]. By using this scheme, authors has demonstrated 16-channel pulse carving [5]. Although over 40 wavelength channels with 2.5 Gb/s repetition rates and 100 GHz channel spacing is feasible in this scheme, rapid pulse broadening in normal dispersion regime limits reaching higher channel counts and larger spectral broadening. This rapid temporal broadening also limits the supercontinuum (SC) generation in normal dispersion regime at higher repetition rates due to interference between adjacent pulses.

Short pulse generation based on spectral slicing of the SC generated in optical fibers is another technique to obtain a DWDM source. Although the SC generation has been used for different applications before, only recently has it been proposed as a DWDM source [6]–[8]. Multiple wavelength pulse sources with more than 100 nm spectral bandwidth generated in specially designed long fibers (>1 km) have been demonstrated by different groups [9], [10]. In an updated work, Kawanishi *et al.* has recently demonstrated propagation of 19 wavelength channels carved out of SC through 40 km of dispersion-shifted (DS) fiber at 160 Gb/s [11]. Each 160 Gb/s channel is generated by 16 times multiplication of pulses carved from the SC. However, since these experiments use long lengths of fibers to generate the SC by adiabatic soliton compression effect, low input power is required, and this requirement leads to lower power spectral density and signal-to-noise ratio (SNR) at the output. Experimental demonstrations reveal that only less than −7 dBm/nm power spectral density is available at the fiber output in long fiber SC generation schemes [12]. In order to compensate low power spectral density, low noise amplifiers are required for long distance propagation. In addition to the issue of power spectral density, Nakazawa *et al.* has shown that the quality of SC generated in long fibers is also limited by the coherence degradation of the channels away from the pump wavelength [13]. In their recent work, the authors show that quality of the SC is correlated with its coherence, and the coherence is degraded by the spreading of amplified spontaneous

Manuscript received March 16, 2000; revised August 30, 2000. This work was supported by DARPA.

Ö. Boyraz, J. Kim, and M. N. Islam are with the EECS Department, University of Michigan, Ann Arbor, MI 48109 USA.

F. Coppinger and B. Jalali are with the Electrical Engineering Department, University of California, Los Angeles, CA 90095 USA.

Publisher Item Identifier S 0733-8724(00)10538-9.

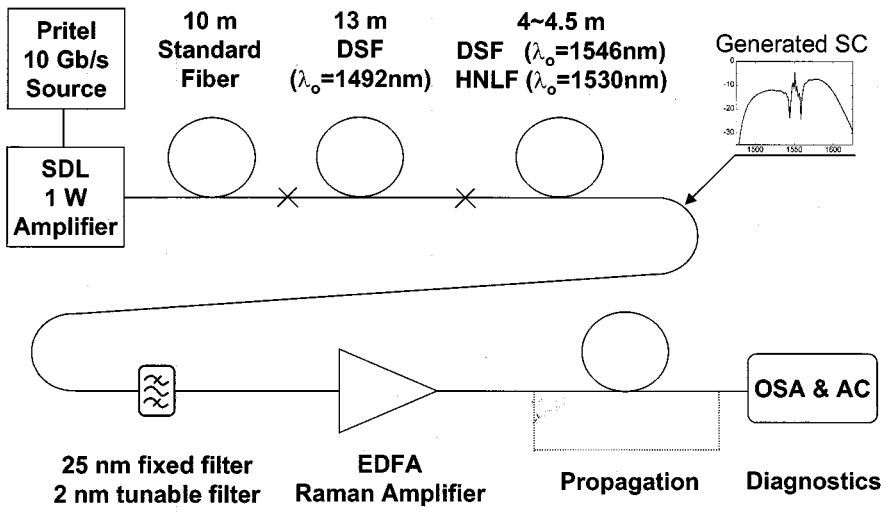


Fig. 1. Experimental setup used for 10 Gb/s SC generation in short fibers. Amplified 10 Gb/s pulse train propagated through three sections of fibers to generate 140 nm SC. Pulse carving followed by amplification and propagation is demonstrated at the EDFA band and at shorter wavelengths. DSF: Dispersion shifted fiber, HNLF: high nonlinearity fiber, OSA: optical spectrum analyzer, AC: autocorrelator.

emission (ASE) noise due to modulation instability (MI) and four wave mixing (FWM) during SC generation.

In this paper, we show that short fiber SC generation has the ability to generate a DWDM source with broad and uniform bandwidth, high-power spectral density, and high coherence. Experimentally, we demonstrate a 10 Gb/s multiple wavelength pulse source with $>$140 nm spectral bandwidth and $\pm$0.5 dB uniformity over 40 nm. The power spectral density is measured to be $+$7.9 dBm/nm across the flat region. Furthermore, the SC can be improved up to 250 nm bandwidth and $\pm$0.5 dB uniformity over 83 nm by using high nonlinearity fibers. Experimental demonstration of $\sim$1.4 ps transform-limited pulse carving as far as 60 nm away from the pump wavelength, pulse propagation and longitudinal mode carving for CW generation indicates that the coherence of the SC is maintained. Based on the theoretical calculations, we also show that the coherence of the short fiber SC generation is maintained, and it has 13 dB higher modulation depth of longitudinal modes as compared to SC generated in long fibers. The experimental and the theoretical results indicate that by using DWDM source based on short fiber SC generation, $>$ 600-channel data transmission with $>$6 Tb/s capacity is achievable at 50 GHz channel separation.

The outline of the paper is as follows. In Section II, we will describe the experimental setup used for SC generation and the experimental results including the generated SC and coherence test based on pulse carving and propagation. We will simulate short fiber SC generation and contrast ratio degradation of longitudinal modes due to noise amplification in Section III. Section IV contains a discussion of possible system applications of the short fiber SC generation as a DWDM source and its advantages. Finally, Section V summarizes our findings.

## II. Experimental Setup and Results of the SC Generation

The experimental setup used in SC generation is shown in Fig. 1. A 10 Gb/s actively modelocked fiber laser generates hyperbolic secant pulses with 1.3 ps temporal width with a time-bandwidth product of 0.32 at 1551 nm. Since the SC is generated in short fibers, $\sim$100 W input peak power is required to achieve enough spectral broadening. We use an erbium-doped fiber amplifier with 30 dBm saturated output power to reach an average power level of 1 W. Following the amplifier, three sections of fibers are used to generate the SC. In general, the first two sections are used for pulse compression and the last section is used for SC formation. Specifically, the first section is 10 m of Corning SMF-28 fiber, where the amplified pulses are compressed via the soliton effect pulse compression. Further pulse compression is obtained by the same effect in DSF1, which is 13 m of DS fiber with $\lambda_0 = 1492$ nm. The last section is 4.5 m of dispersion shifted fiber (DSF2) with $\lambda_0 = 1546$ nm or 4 m of high nonlinearity dispersion shifted (HNL-DS) fiber with $\lambda_0 \sim 1530$ nm. The third-order dispersion is the dominant effect in this section, and spectral flattening accompanied by additional spectral broadening is obtained [14], [15]. Since the first two sections of fibers are the same, throughout the paper, we differentiate the two SC setups according to the fiber used in the last section. Table I summarizes the fiber parameters used in the experiment. Detailed description of the mechanisms contributing to the SC generation will be discussed in the next section. We demonstrate spectral slicing for short pulse generation both within the EDFA band and at shorter wavelengths by using a 2.3-nm tunable filter. A 25-nm super-Gaussian filter centered at 1490 nm is used for testing the broadband coherence. After the amplification of the pulses carved at short wavelengths by a Raman amplifier, 26 km of Corning SMF-28 fiber is used for propagation. An optical spectrum analyzer with 6.25 GHz spectral resolution and an autocorrelator are used for diagnostics.

Fig. 2(a) shows the 10 Gb/s SC spectra generated in conventional, low nonlinearity, DS fiber. We obtain 140 nm spectral broadening at 20 dB below the spectral peak. The SC has three regions where most of the energy is accumulated: 1) center, 2) Stokes. and 3) anti-Stokes regions. The Stokes side has 44 nm

TABLE I

| Fiber | Section | Length (m) | $\lambda_0$ (nm) | $\partial D/\partial\lambda$ ($ps^2$/nm.km) | $\gamma$ ($W^{-1}.km^{-1}$) |
|---|---|---|---|---|---|
| SMF-28 | 1 | 10.0 | 1310 | 0.076 | 2.3 |
| DSF-1 | 2 | 13.0 | 1492 | 0.03889 | 2.3 |
| DSF-2 | 3 | 4.5 | 1546 | 0.05557 | 2.3 |
| HNL-DSF | 3 | 4.0 | 1530 | 0.0265 | 9.9 |

bandwidth at 15 dB below the center peak, and 20 nm spectral region with $\pm$0.5 dB uniformity. The power spectral density in this region is measured to be 11 dBm/nm. On the other hand, the anti-Stokes side has 50 nm bandwidth at the same level and 40 nm spectral region with the same uniformity of $\pm$0.5 dB. Unlike the Stokes region, power spectral density in this side is lower, 7.9 dBm/nm. A generated SC with a nearly symmetric spectrum indicates that the spectral broadening mechanism is dominated by self-phase-modulation (SPM) during the SC generation. A 6 nm difference in bandwidth and 3 dB difference in power density shows the effect of third-order dispersion, which leads to asymmetrical flattening of the anti-Stokes side while lowering the power spectral density. The center part of the SC has the peak spectral density and 16 nm bandwidth.

The spectral broadening is increased to 250 nm by replacing the last section of the SC fiber with HNL-DS fiber. Experimentally, we use 4 m of HNL-DS fiber with 4.5 times higher nonlinearity and zero dispersion wavelength at 1530 nm to replace DSF2. Similar SC to that obtained from DSF2 is generated, but due to the higher nonlinearity and lower dispersion slope in the HNL-DS fiber, spectral broadening is increased to 250 nm [16]. Fig. 2(b) shows the generated SC spectra with 250 nm bandwidth in high nonlinearity fiber. The flat region on the anti-Stokes side is increased to 83 nm with the same $\pm$0.5 dB uniformity. However, because of the lower input power requirement due to increased nonlinearity, almost doubled spectral broadening, and higher splice loss, the power spectral density of the flat region is decreased to 0 dBm/nm at the flat portion of the spectrum. The bandwidth of the Stokes region is measured to be 21 nm with $\pm$0.5 dB uniformity and 9 dBm/nm power spectral density.

The coherence of the SC is tested by measuring the pulse quality across the spectrum and by carving longitudinal modes to generate CW light. The SC generation setup with conventional DS fiber is used for pulse carving and coherence measurements. Experimentally, we use two different filters to carve out pulses across the spectrum. The first filter is a tunable Gaussian filter with a tuning range of 70 nm from 1490 nm to 1560 nm and nominally 2.3 nm bandwidth, which varies from 2.4 nm to 2 nm within the tuning range. The second filter is a 25-nm super-Gaussian filter centered at 1490 nm. In the first step of the experiment, we test the coherence of the pulses carved from SC near the EDFA band. We use the tunable filter to carve out a

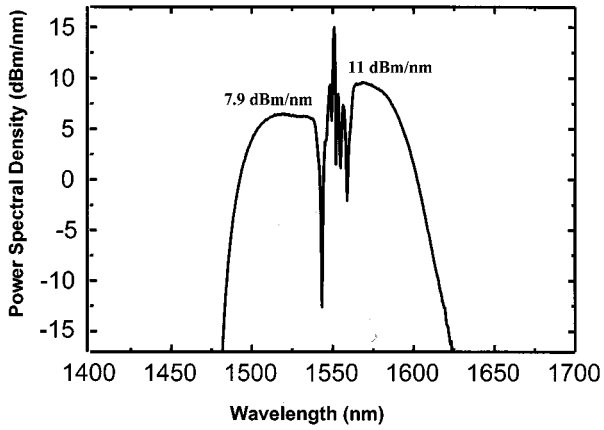


(a)

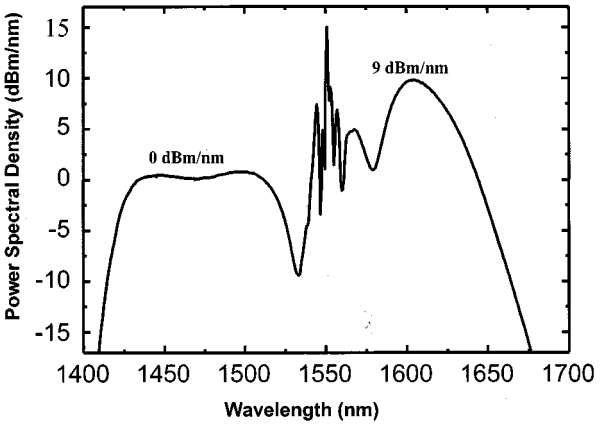


(b)

Fig. 2. (a) SC spectra generated in conventional DS fibers. We measure 140 nm bandwidth with $\pm$0.5 dB uniformity over 40 nm. Power spectral density is measured to be 7.9 dBm/nm over the flat region. (b) The spectral broadening improved to 250 nm with $\pm$0.5 dB uniformity over 83 nm by using high nonlinearity DS fibers.

pulse at 1524.8 nm with 2.11 nm 3 dB bandwidth, as shown in Fig. 3(a). In order to check the nonlinear behavior of the carved pulses, we propagate it through 12 km of dispersion shifted fiber with $\lambda_0 = 1524$ nm. Fig. 3(b) shows the pulse spectra after the propagation for three different average input power levels of 1 mW, 3 mW, and 5 mW. Since the carved pulse is very close to zero-dispersion-wavelength, SPM-dominated propagation characteristics are presented at the output of the fiber. The number of the spectral peaks indicate nonlinear phase shift of $\sim\pi$, and $\sim 2.5\,\pi$ is obtained for input power levels of 3 mW and 5 mW, respectively. The asymmetry in the spectrum is expected due to normal dispersion effect at shorter wavelengths. These results show that the temporal stability and the coherence of the SC within EDFA band are preserved.

In the second step of the coherence test, we carve pulses near 1500 nm and propagate through 26 km SMF fiber after amplification. We use a Raman amplifier to amplify the signal after carving pulses at short wavelengths and before propagation. The Raman amplification is obtained by using two sections of dispersion shifted fibers with 4.4 km length and a CW pump source at 1117 nm. Accumulated chirp in the Raman

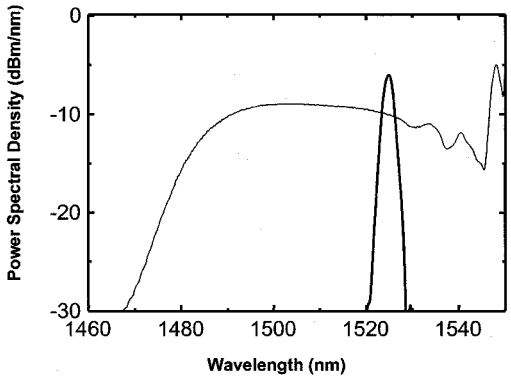


(a)

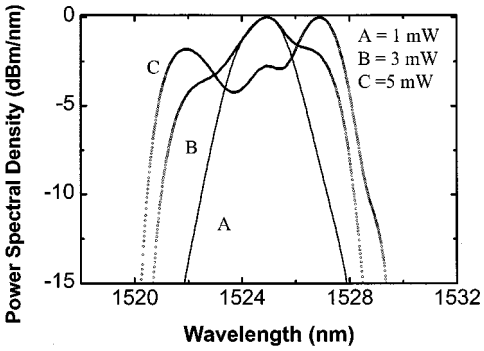


(b)

Fig. 3. (a) Transform limited pulse carving has been demonstrated vicinity of the EDFA band (1524 nm). (b) We check the propagation behavior of the carved pulses by propagating through 12 km DS fiber for three different input power levels. SPM dominated spectral modulation indicates that spectral carving of the SC near EDFA band generates soliton like pulses and coherence of the SC is maintained.

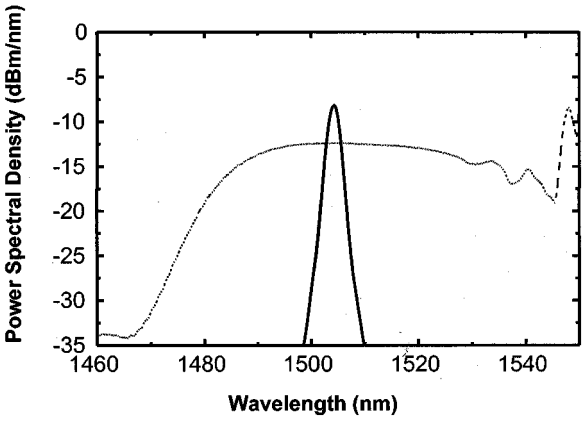


(a)

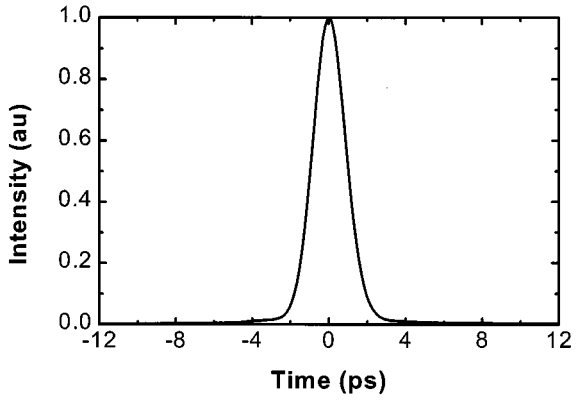


(b)

Fig. 4. (a) Transform limited pulse carving is demonstrated near 1500 nm. (b) The autocorrelation trace of the carved pulse at 1504 nm. We obtain 1.37 ps nearly transform limited Gaussian pulses with time-bandwidth product of $\sim$0.45.

amplifier is compensated by using a 2.5 km of SMF-28 fiber after the amplifier. Optimum chirp compensation is obtained at $\sim$1504 nm. After compensation, we carve 1.37 ps nearly transform limited Gaussian pulses with $\Delta\tau\Delta\nu = 0.45$ at 1504 nm indicated in Fig. 4(a). The corresponding autocorrelation trace is shown in Fig. 4(b). The coherence of the pulse is confirmed by the propagation through 26 km of SMF-28 fiber. Because of the very high dispersion, which is more than 700 ps, a higher repetition rate pulse train is observed in the temporal domain at the output end of the SMF-28 fiber. The phenomenon of obtaining high repetition pulses in linear propagation is explained by longitudinal mode beating resulted from high dispersion [17]. Shake *et al.* show that, because of dispersion, a pulse is formed at the time position where longitudinal modes of the several adjacent pulses overlap. With further dispersion, the repetition rate decreases gradually and returns to fundamental operation frequency. The autocorrelation of the propagation results are shown in Fig. 5. The separation between adjacent pulses are measured to be $\sim$21 ps, which corresponds a pulse train at 48 GHz repetition rate. The pulse train remains stable as long as environmental fluctuations are isolated. This measurement result indicates that the longitudinal mode structure of the laser is replicated across the SC instead of incoherent energy spreading, which also shows that the coherence of the SC is preserved.

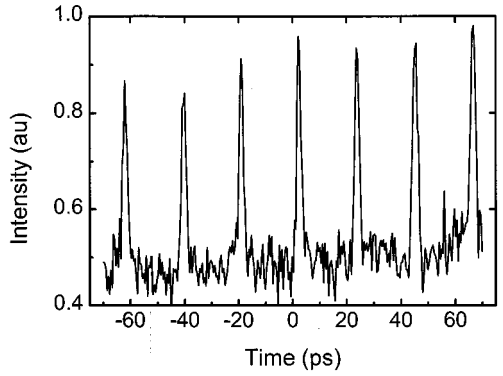


Fig. 5. High repetition rate pulse train is obtained after propagating the carved pulses through 26 km of standard fiber. More than 700 ps dispersion leads to beating of the longitudinal modes at different time position and creates 48 GHz pulse train.

The pulse carving results across the whole Raman gain bandwidth are shown in Fig. 6(a). In addition to pulse carving and propagation at single wavelength in Raman gain bandwidth, we demonstrate carvability of the SC spectra wavelengths between 1490 nm and 1511 nm. Since the chirp compensation is optimized for the wavelength 1504 nm, broader pulse widths are

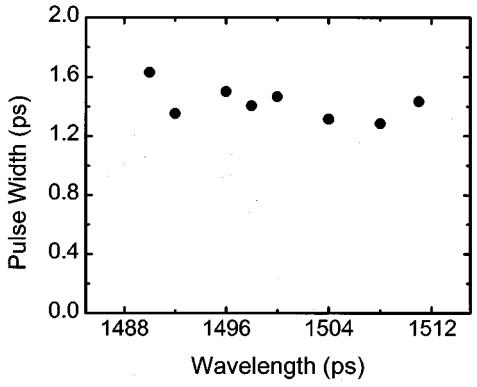


(a)

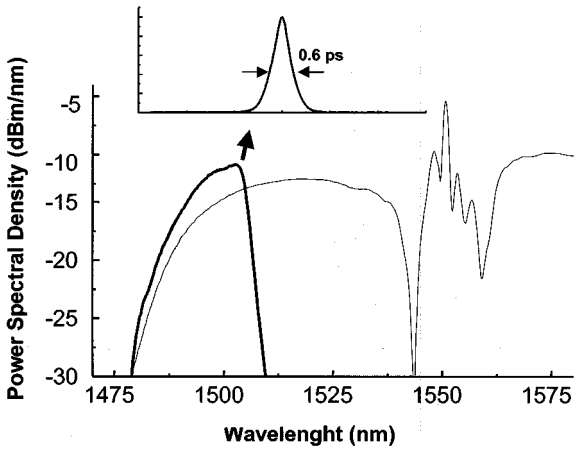


(b)

Fig. 6. (a) Results of the coherent pulse carving after subtracting the total dispersion in the 11 km of DSF at the Raman amplifier. Nearly transform limited pulses are generated with average $\tau \sim 1.5$ ps and $\Delta\tau\Delta\nu \sim 0.46$. The results indicate that the coherence of the SC is maintained up to 60 nm away from the pump and it is uniform across the spectrum. (b) A 0.6 ps short pulse carving with 20 nm broadband filter shows the coherence of the SC is maintained even at the edge of the SC.

measured at wavelengths other than 1504 nm. After subtracting the pulse broadening during the amplification by using the formula $\tau = \tau_{meas} - (\lambda_0 - \lambda_c) \cdot \Delta\lambda \cdot \partial D/\partial\lambda \cdot L$, we calculate the actual width of the carved pulses. The parameter $\tau_{meas}$ is the measured pulsewidth, $\lambda_0$ is zero dispersion wavelength of the fiber, $\lambda_c$ is pulse carving wavelength, $\Delta\lambda$ is the filter bandwidth, $\partial D/\partial\lambda$ is the dispersion slope, and $L$ is the fiber length in the Raman amplifier. Fig. 6(a) shows the calculated pulse widths after subtracting the effect of the total dispersion accumulated in the amplifier from the measured pulse widths. An average of ~1.5 ps pulse width and $\Delta\tau\Delta\nu \sim 0.46$ indicates that the coherence of the SC is preserved up to 60 nm away from the pump wavelength and uniform across the spectrum. As another example, Fig. 6(b) shows the generation of 0.6 ps pulses with 20 nm spectral carving, which also indicates that coherence is preserved even at the edge of the SC. The inconsistency between filter bandwidth and the pulse width arises because the edge of the SC spectrum does not completely fill the filter bandwidth and the pulses are slightly chirped before the autocorrelator.

The coherence of the SC is also confirmed by CW generation by longitudinal mode carving of the generated SC. In an

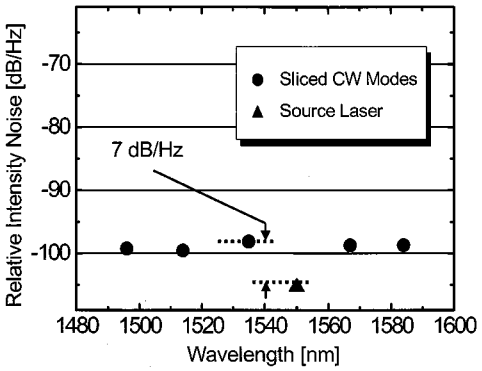


Fig. 7. Experimental results of relative intensity noise measurement. The results indicate that the longitudinal modes of the pump are replicated with 7 dB/Hz noise degradation. The results also show that each of the longitudinal modes can be carved to generate a CW signal. Uniformity of relative intensity noise shows that coherence is preserved equally across the SC.

updated experiment, we have demonstrated that longitudinal modes of the SC can be carved to generate CW light [18]. The carving results indicate that the longitudinal modes of the seed pump source is replicated during the SC generation with low noise degradation. As a figure of merit, we measure the noise performance of CW from the SC and CW from seed pump. Fig. 7 shows the measured relative intensity noise for CW signals carved from the pump and the SC. The measurement results show that the generated CW source has less than 7 dB/Hz intensity noise degradation across the spectrum compared to the pump. This degradation is attributed to the amplifier noise, ASE noise, and MI effects during SC formation. However, the uniformity of the intensity noise shows that coherence of the SC is preserved equally across the spectrum.

## III. Mechanisms of SC Generation and Theoretical Results

We confirm our experimental results by simulating the SC generation. We also focus on the evolution of the SC starting with the amplifier output and discuss the behavior of the spectral broadening with respect to linear and nonlinear effects in the fiber. The generation of SC is modeled by the nonlinear Schrodinger equation, which describes the pulse propagation under the influence of nonlinear and linear effects in the fiber. The equation is formulated as

$$\frac{\partial U}{\partial z} + \frac{i}{2}\beta_2\frac{\partial^2 U}{\partial t^2} - \frac{1}{6}\beta_3\frac{\partial^3 U}{\partial t^3} = i\gamma\left[|U|^2 + \frac{2}{3}|U_x|^2 - T_R\frac{\partial |U|^2}{\partial t}\right]U$$

where $U$ defines the normalized envelope function of the electric field at the main axis and $U_x$ defines the component at the orthogonal polarization [19]. The left side of the equation gives the linear pulse propagation under the influence of group velocity dispersion (GVD) and third-order dispersion (TOD), where $\beta_2$ is the second-order dispersion constant (ps$^2$/km) and $\beta_3$ is the TOD constant (ps$^3$/km). The perturbations caused by the nonlinear effects in the fiber are given by the terms on the right-hand side of the equation. The first two nonlinear terms on the right side are SPM and cross phase modulation (XPM) effects, and the stimulated Raman scattering is included as the last term on

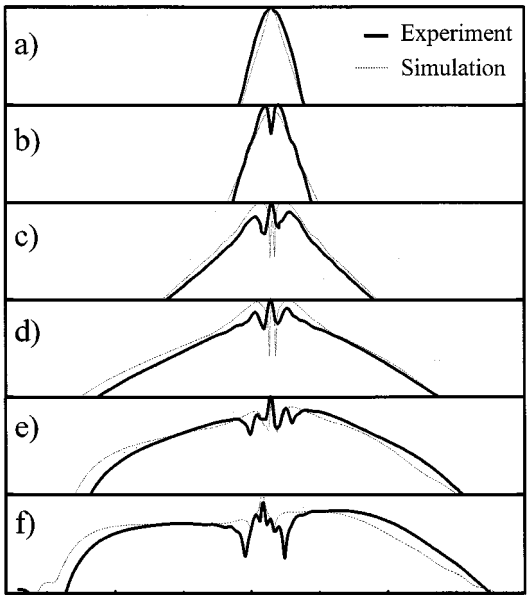


Fig. 8. Experimental and simulation results of the SC generation in optical fibers based on the experimental fiber parameters. This figure shows the evolution of SC spectra at fiber lengths of (a) after the amplifier, (b) 10 m, (c) 23 m, (d) 24.5 m, (e) 26 m, and (f) 27.5 m. The straight line shows the experimental results and dotted line shows the simulation results.

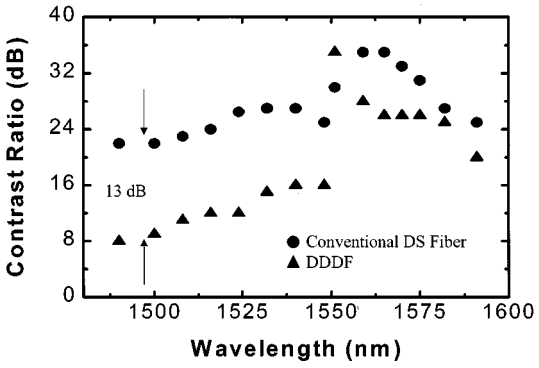


Fig. 9. Simulation results of the coherence degradation in short fiber SC generation and 1 km of dispersion decreasing and dispersion flattened fiber (DDDF). • indicates modulation depth (contrast ratio) of longitudinal modes calculated for SC generated in short DS fibers, and ▲ shows the contrast ratio calculated for the SC generated in long DDDF fibers. In average, short fiber SC generation has ∼13 dB higher contrast ratio than the one generated in 1 km fiber.

the right-hand side. The nonlinearity constant is defined by $\gamma$ ($W^{-1}km^{-1}$). Raman gain is defined by the constant $T_R$, which is set to be 5 fs. We use the split step Fourier method to simulate the SC generation [19].

Fig. 8 summarizes the evolution of the SC generation based on fiber parameters used in the experiment. Fig. 8(a) shows the pulse spectrum after the amplifier. Due to >20 m of gain fiber and patch cords, the spectral width of the pulse at the amplifier output is increased from 2 nm to 3.2 nm, which shows that the pulse compression starts during the amplification. At the end of the 10 m of SMF-28 fiber, we observe soliton effect pulse compression with a clear indication of SPM, as shown in Fig. 7(b). The double peak on the spectrum indicates that signal acquires nearly $3\pi/2$ nonlinear phase shift in the first section. Fig. 8(c) shows the spectral broadening at the end of the DSF1 fiber. Since the GVD is nearly four times smaller in the second section than the first section, higher nonlinear phase shift is acquired. The contribution of the TOD is also expected to appear with increasing bandwidth in this section and to cause small spectral asymmetry. The spectral flattening occurs in the last section of the fiber, where GVD is as low as 0.3 ps/nm.km. Although the spectral broadening still continues along the fiber in this section, spectral asymmetry also continues to grow with increasing TOD effect due to large bandwidth. Fig. 8(d) shows the shape of the spectrum at one-third of the length of the last section, where TOD effects starts to show up more clearly. Starting with the second half of the DSF2, asymmetric pulse break up starts to dominate at the trailing end of the pulse and the rate of the spectral broadening decreases. However, the rate of spectral flattening increases with the pulse breakup and anti-Stokes side becomes wider and flatter. Fig. 8(e) shows the power spectral density distribution at 3 m of DSF2 fiber. Complete flattening is obtained at the last 1.5 m of DSF2 fiber, as seen in Fig. 7(f). The simulation results show that the contribution of Raman in SC generation is minimal, and this can be explained by the shortness of the fiber.

We calculate the degradation in phase coherence during the SC generation by using the same simulation. Since there is no direct measurement of coherence for pulsed laser, we use SNR, i.e., the depth of longitudinal modes, as an indicator for the coherence. Our aim is to measure how much the SNR and depth of longitudinal modes degrade compared to input signal due to interaction of ASE noise with signal during SC generation. Deteriorating SNR values shows increasing randomness in phase and amplitude due to ASE noise. In previous works, this comparison has been demonstrated for different combinations of long fiber SC generation, and it has been shown that the coherence degradation due to ASE amplification is less in dispersion decreasing fibers than in constant dispersion fibers and dispersion flattened fibers [13]. For comparison, we simulate the SC generation in short fibers with experimental parameters as well as in dispersion-decreasing-dispersion-flattened (DDDF) fiber. The length of DDDF is set to 1 km with dispersion parameters of $-10.5$ $ps^2/km$ and 0.1 $ps^2/km$ at the beginning and at the end of the fiber, respectively. The soliton order at the beginning of DDDF fiber is set to ∼1.6. In order to simulate the ASE, we generate a background noise with random amplitude and phase generated by a Gaussian random number generator. The initial SNR is set to be 45 dB, which corresponds to an amplifier with noise figure of ∼7 dB. Since the coherence of the pulse is related to the contrast ratio, modulation depth, of the longitudinal modes, we calculate the contrast ratio at different spectral points along the SC for comparison.

Fig. 9 summarizes the calculated contrast ratio at different points along the SC spectra for two different fibers. The simulation results show that the SNR and the modulation depth are degraded more than 20 dB in both fibers due to MI initiated by background ASE. However, the short fiber SC generation shows better contrast ratio compared to the DDDF fiber. Specifically, 13 dB less degradation is calculated in short fiber SC generation

at 60 nm away from the pump, where contrast ratio decreases to as low as 9 dB in DDDF fiber. The only exception is that 4-dB better modulation depth is calculated at the vicinity of the pump wavelength, where long fiber SC has a spectral peak. The asymmetry in contrast ratio degradation is caused by the higher power spectral density at longer wavelengths, and the location of the pump wavelength close to the edge of the EDFA band. Nearly flat contrast ratio ($\sim$22 dB) around 1500 nm also confirms the transform limited pulse carving and broadband coherence demonstrated experimentally.

## IV. Discussion

Our experimental and theoretical results confirm that the DWDM source based on short fiber SC generation satisfies all the requirements of a source used in OTDM/WDM applications. Although synchronization and wavelength accuracy are inherent properties of DWDM sources from a single laser, coherence, bandwidth, uniformity, and high-power spectral density are four main properties that can be satisfied by DWDM source based on short fiber SC generation. By using multiple wavelength pulse generation based on spectral slicing of short fiber SC, we show that the bandwidth of the source can be more than doubled with $\pm$10% amplitude variation over 80 nm compared to chirped pulse modulation and SC generation in normal dispersion fiber. This bandwidth can be increased up to 250 nm by compromising the spectral uniformity and power spectral density. Moreover, for a single-channel DWDM source 10 Gb/s data rate shows nearly two orders-of-magnitude increments in repetition rates without any pulse interleaving circuit compared to sources generated by chirped pulse modulation technique. On the other hand, data encoding on multiple wavelength channels simultaneously by using a single modulator is a unique feature used in chirped pulse modulation technique, where this modulation technique cannot be implemented by using high repetition rate SC sources. However, the channel count is proportional to the speed of the modulator and the amount of chirping. This proportionality limits the operation frequency in chirped pulse modulation technique due to availability of high-speed modulators and inter-pulse interference caused by high chirping. In addition to high bit rate operation, by using the short fiber SC generation scheme in conventional dispersion shifted fibers, the power spectral density is improved by more than 15 dB compared to long fiber SC generation, and bandwidth is uniform over 40 nm. This uniform bandwidth can also be improved to 83 nm at the expense of 8 dB decrease in power spectral density, which still gives 7 dB improvement in power level compared to long fiber SC generation scheme.

Since actual coherence measurements of a pulsed laser by interferometric techniques are limited by frequency chirp and pulsed nature of the signal, spectral carvability, SNR, CW generation by longitudinal mode filtering and propagation characteristics can be used as indicator of coherence [13]. In our experiments, we show that the SC generated in short fibers maintains its coherence up to 60 nm away from the pump wavelength by transform limited pulse carving and propagation within and outside the EDFA band. These results are also confirmed theoretically. We calculate that the pulses carved from the short fiber SC have longitudinal modes contrast ratio of 22 dB even at 60 nm away from the pump wavelength for the input signal with SNR of 45 dB. Compared to the contrast ratio of 9 dB at the same point obtained in long fiber SC generation scheme, short fiber SC generation scheme shows 13 dB improvement in modulation depth of longitudinal modes and in coherence. Although essential mechanisms for spectral broadening in both fibers are the same, the difference between contrast ratio can be explained by the difference in the length. In the short fiber SC generation spectral, flattening occurs within a distance less than half soliton period, where optimum compression is obtained. For soliton orders $<$10, MI perturbation is not as effective as higher order solitons within half soliton period [13]. The stepwise dispersion decreasing pulse compression scheme with relatively high average dispersion ($\sim$9.5 ps/nm.km) is also disturbs MI gain in the first two sections. Although in DDDF fiber, decreasing dispersion profile reduces MI gain, the average dispersion is low and steady growth of ASE noise with increasing gain bandwidth is still expected along the fiber. Moreover, the pulses propagate multiple soliton periods, where the symmetry of initial soliton disappears due to MI.

CW signal generation based on longitudinal mode carving also confirms that the coherence is preserved across the spectrum. The 7 dB/Hz amplitude noise degradation compared to the pump signal shows that generated SC has similar coherence. This 7 dB/Hz difference confirms the degradation due to amplification and MI during SC generation. However, the uniformity of the intensity noise also shows that the coherence is maintained equally across the whole SC spectra. In addition to coherence, power spectral density of the two scheme is compared. Since SC generation in long fibers depends on adiabatic soliton compression effect, where this compression scheme requires low input power, the low power spectral density ($-$7 dBm/nm) and low SNR is obtained at the output. These results lead to high amplification requirement at the output, where no single amplifier module is available to cover the whole SC bandwidth.

To understand the capacity of SC generation, we calculate the maximum achievable number of channels by assuming 50 GHz (0.4 nm) filter spacing, which is commercially available. Our experimental results indicate that SC generation in high nonlinearity fibers has the capacity of achieving $>$200 wavelength channels at 10 Gb/s over 83 nm bandwidth with $\pm$0.5 dB amplitude uniformity. Due to overall bandwidth of 250 nm, these capacities can reach up to 6 Tb/s by utilizing the entire SC bandwidth at the expense of amplitude equalization circuit. Compared to the experimental demonstration of 235 Gb/s by using chirped pulse modulation technique, short fiber SC generation has the capability of an order of magnitude improvement without any pulse interleaving circuit.

## V. Summary

In summary, we demonstrate coherent short pulse generation based on spectral slicing of the SC generated in short fibers at 10 Gb/s. By using conventional DS fibers, we generate 140 nm spectral broadening with 7.9 dBm/nm ($\pm$0.5 dBm) power spectral density over 40 nm. By using high nonlinearity dispersion shifted fibers, spectral broadening is improved to 250 nm with

$\pm 0.5$ dB uniformity over $>80$ nm. Coherence of the SC is tested by pulse carving, propagation and longitudinal mode carving. The results show that the coherence of the short fiber SC generation is maintained up to 60 nm away from the pump wavelength. We confirm our results by calculating the SNR degradation because of interaction of pulses with ASE noise during the SC generation. The simulation results show that the longitudinal mode contrast ratio of the pulses carved from the SC degrades nearly 23 dB at 60 nm away from the pump wavelength. The 13 dB improvement in contrast ratio is calculated at 60 nm away from pump compared to the results obtained by using long fiber SC generation. As a DWDM source short fiber SC source can also improve the power spectral density by $>15$ dB compared to the SC generated in long fibers. Compared to the chirped pulse modulation technique, we obtain doubled uniform spectral bandwidth at $>200$ times higher repetition rates. Based on the experimental results, we estimate that synchronous 600 wavelength channels with total of $>6$ Tb/s data rate at 50 GHz channel spacing is achievable by utilizing the 250 nm spectral bandwidth generated in high nonlinearity fibers.

## ACKNOWLEDGMENT

The authors would like to thank Dr. M. Freeman from Xtera Communications, Inc. for lending and setting up the Raman amplifier.

## REFERENCES

[1] E. A. De Souza, M. C. Nuss, W. H. Knox, and D. A. B. Miller, "Wavelength-division multiplexing with femtosecond pulses," *Electron. Lett.*, vol. 20, no. 16, pp. 1166–1168, 1995.

[2] M. C. Nuss, W. H. Knox, and U. Koren, "Scalable 32 channel chirped-pulse WDM source," *Electron. Lett.*, vol. 22, no. 20, pp. 1311–1312, 1996.

[3] L. Boivin, M. Wegmueller, M. C. Nuss, and W. H. Knox, "110 Channels $\times$ 2.35 Gb/s from a single femtosecond laser," *IEEE Photon. Technol. Lett.*, vol. 11, no. 4, pp. 466–468, 1999.

[4] B. Mikulla, L. Feng, S. Sears, B. C. Collings, M. Arend, and K. Bergman, "Broad-band high-repetition-rate source for spectrally sliced WDM," *IEEE Photon. Technol. Lett.*, vol. 11, no. 4, pp. 418–420, 1999.

[5] B. Mikulla, L. Feng, S. Sears, M. Arend, and K. Bergman, "16 Channel $\times$ 2.5 Gbit/s WDM source using an harmonically and passively mode-locked Er/Yb fiber laser," in *IEEE/LEOS Annu. Meet. 1998*, paper WT1.

[6] K. Mori, T. Morioka, and M. Saruwatari, "Group velocity dispersion measurement using supercontinuum picosecond pulses generated in an optical fiber," *Electron. Lett.*, vol. 29, no. 11, pp. 987–989, 1993.

[7] H. Takara, S. Kawanishi, T. Morioka, K. Mori, and M. Saruwatari, "100 Gb/s optical waveform measurement with 0.6 ps resolution optical sampling using subpicosecond supercontinuum pulses," *Electron. Lett.*, vol. 30, no. 14, pp. 1152–1153, 1994.

[8] T. Morioka, K. Mori, S. Kawanishi, and M. Saruwatari, "Multi-WDM-channel, Gbit/s pulse generation from a single laser source utilizing LD-pumped supercontinuum in optical fibers," *IEEE Photon. Technol. Lett.*, vol. 6, no. 3, pp. 365–368, 1994.

[9] K. Mori, H. Takara, S. Kawanishi, M. Saruwatari, and T. Morioka, "Flatly broadened supercontinuum spectrum in a dispersion decreasing fiber with convex dispersion profile," *Electron. Lett.*, vol. 33, no. 21, pp. 1806–1807, 1997.

[10] T. Okuno, M. Onishi, and M. Nishimura, "Generation of Ultra-broad-band supercontinuum by dispersion-flattened and decreasing fiber," *IEEE Photon. Technol. Lett.*, vol. 10, no. 1, pp. 72–74, 1998.

[11] S. Kawanishi, H. Takara, K. Uchiyama, I. Shake, and K. Mori, "3 Tb/s (160 Gbit/s $\times$ 19 ch) OTDM/WDM transmission experiment," in *OFC'99*, 1999, paper PD1-1.

[12] T. Morioka, S. Kawanishi, H. Takara, O. Kamatani, M. Yamada, T. Kanomori, K. Uchiyama, and M. Saruwatari, "100 Gbit/s $\times$ 4 ch, 100 km repeaterless TDM-WDM transmission using a single supercontinuum source," *Electron. Lett.*, vol. 32, no. 5, pp. 468–470, 1996.

[13] M. Nakazawa, H. Kubota, and K. Tamura, "Random evolution and coherence degradation of a higher-order optical soliton train in the presence of noise," *Opt. Lett.*, vol. 24, no. 5, pp. 318–320, 1999.

[14] G. A. Nowak, J. Kim, and M. N. Islam, "Stable 200 nm TDM/WDM source based on continuum generation in 2 m of fiber," in *OFC'99*, 1999, paper TuB3-1.

[15] ——, "Stable supercontinuum generation in short length of conventional dispersion-shifted fiber," *Appl. Opt.*, vol. 38, no. 36, pp. 7364–7369, 1999.

[16] J. Kim, G. A. Nowak, O. Boyraz, and M. N. Islam, "Low energy, enhanced supercontinuum generation in high nonlinearity dispersion-shifted fibers," in *CLEO'99*, 1999, paper CWA7.

[17] I. Shake, H. Takara, S. Kawanishi, and M. Saruwatari, "High-repetition-rate optical pulse generation by using chirped optical pulses," *Electron. Lett.*, vol. 34, no. 8, pp. 792–793, 1998.

[18] J. Kim, Ö. Boyraz, and M. N. Islam, "$150^{+}$ channel ultra-DWDM source with $N \times 10$ GHz spacing utilizing longitudinal mode slicing of supercontinuum," in *OFC'00*, 2000, paper ThA2.

[19] G. P. Agrawal, *Nonlinear Fiber Optics*, 2nd ed. New York: Academic, 1995.

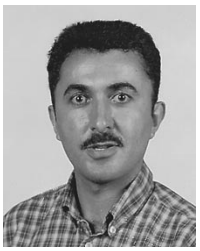

**Ö. Boyraz** received the B.S. degree in electrical engineering from the Hacettepe University, Turkey, in 1993 and the M.S. degree in electrical engineering from the University of Michigan, Ann Arbor, in 1997. He is currently pursuing the Ph.D. degree in electrical engineering at the University of Michigan.

His research areas include linear and nonlinear aspects of fiber optics communication systems. His Ph.D. study includes experimental study of all-optical switching and access node design, optical WDM sources, and optical analog to digital conversion.

Mr. Boyraz has been awarded with full scholarship by the Turkish government for his graduate studies. He is a student member of the Institute of Electronic and Electrical Engineers.

**J. Kim** received the B.S. degree in electrical engineering from Kwangwoon University, Seoul, Korea in 1992 and the M.S. degree in electrical engineering from the University of Arizona, Tucson, in 1994. Since 1997, he has been pursuing the Ph.D. degree in electrical engineering at the University of Michigan, Ann Arbor, were he is an EECS Department Fellow.

From 1995 to 1997, he a Research Engineer at the Institute for Advanced Engineering, Seoul, Korea, where he was involved in research and development of laser/fiber-optic gyroscopes. Currently, he is an Research Assistant in Integrated Optics Laboratory at the University of Michigan. His research interest include linear and nonlinear aspects of fiber optics, design, simulation, fabrication of integrated optic devices, and utilization of them in optical transmission systems.

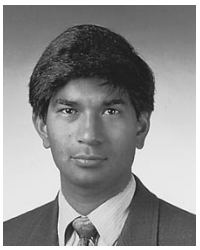

**M. N. Islam** received the B.S. degree in 1981, the M.S. degree in 1983, and the Sc.D. degree in 1985, all in electrical engineering, from the Massachusetts Institute of Technology, Cambridge.

From 1985 to 1992, he was a Member of the Technical Staff in the Advanced Photonic Department at AT&T Bell Laboratories, Holmdel, NJ. He joined the EECS Department at the University of Michigan, Ann Arbor, in 1992, where he is currently a full tenured Professor. He has published over 95 papers in refereed journals and holds over 25 patents. In addition, he has founded two spin-off companies from the University of Michigan—AccuPhotonics and Bandwidth Solutions.

Prof. Islam was a Fannie and John Hertz Fellow from 1981 to 1985, and in 1992, he was awarded the OSA Adolf Lomb Medal for pioneering contributions to nonlinear optical phenomena and all-optical switching in optical fibers. He also received the U-M Research Excellence Award in 1997 and became a Fellow of the Optical Society of America in 1998.

**F. Coppinger**, photograph and biography not available at the time of publication.

**B. Jalali** (SM'97) from 1988 to 1992, he was a Member of Technical Staff at the Physics Research Division of AT&T Bell Laboratories, Murray Hill, NJ, where he conducted research on ultrafast electronics and optoelectronics. He was responsible for successful development and delivery of 10 Gb/s lightwave circuits to U.S. Air Force in 1992. Currently, he is a Professor of Electrical Engineering and the Chair of the Photonics and Optoelectronics field at the University of California, Los Angeles. He is the director of the DARPA Consortium for Optical A/D System Technology (COAST). His current research interests are in microwave photonics, integrated optics, and photonic sensors. He has over 150 publications and holds four patents.

Dr. Jalali is the Vice Chair of the IEEE LEOS Los Angeles chapter, the General Chair for the 2001 IEEE Microwave Photonics Conference, a member of the Optical Society of America (OSA), and Eta Kappa Nu. He is a consultant for NASA/JPL and several fiber-optic companies and sits on the Board of Directors of Cognet Microsystems, Inc.